Automation in Construction 119 (2020) 103303

Contents lists available at ScienceDirect

Automation in Construction

journal homepage: www.elsevier.com/locate/autcon

Sampling robot for primary circuit pipelines of decommissioned nuclear facilities

Michal Starý[a,*], František Novotný[a], Marcel Horák[a], Marie Stará[b]

[a] Institute for Nanomaterials, Advanced Technologies and Innovation, Technical University of Liberec, Studentská 1402/2, 461 17 Liberec 1, Czech Republic
[b] Faculty of Mechanical Engineering, Technical University of Liberec, Studentská 1402/2, 461 17 Liberec 1, Czech Republic

ARTICLE INFO

Keywords:
Decommissioning
Nuclear power plant
Service robot
Sampling probe
Radioactive contamination

ABSTRACT

Nuclear power plants, as one of the cornerstones of today's global and, most importantly, European energy sector, place considerably high demands on all stages from design and construction, through operation and control, to safe decommissioning at the end of the facility's life. A relatively large decommissioning process is underway in Europe, which will increase over the coming decades. This process of decommissioning nuclear facilities is closely linked to the objective assessment of the efficiency of decontamination processes. The present paper deals with techniques and technologies for obtaining samples from the hard-to-reach inner surface of the primary circuit of a nuclear reactor. Sampling by a service robot fitted with sampling probes is assumed to be performed under relatively dry conditions, i.e. before the application and after the discharge of the decontamination solution. The basis of the electro-pneumatic robot for default pipes with a diameter of 500 mm is an eight-wheel mobile platform with self-stabilizing capability thanks to inclined wheels. The robot is equipped with a pair of unique sampling probes and a fixing arm to position the robot in the pipeline during the sampling. The basis of the article is the technical solution of the service robot, with an emphasis on the functioning and efficiency of the sampling probes. The presented comprehensive system constitutes a proven knowledge base for the decommissioning of nuclear power facilities.

1. Introduction

Nuclear power is one way of meeting society's energy needs. Currently, more than 450 nuclear power reactors are in operation around the world and another 54 are under construction [1]. Although the future of the reactor core is now being discussed again in a number of countries as a source for power generation, it is necessary, despite the outcome, to provide a controlled and safe decommissioning process for each nuclear block after the end of its operation. The originally planned duration of operation of the first-generation nuclear power plants (NPPs) was 30 years [2]. Due to modern technologies and advanced diagnostic methods, the lifespan can be increased based on current estimates to 60 years and more [3,4]. A massive decommissioning process is already underway in Europe [5–7], which is perhaps the most advanced in the Soviet-type WWER-440 power plant in Greifswald in the east of Germany. This power plant was shut down in 1995 and now serves as an example for the decommissioning of other NPPs of the respective type [8–10].

NPPs around the world are most often based on the technology of a pressurized light-water moderated and cooled reactor (PWR) [11], which in the Russian version is referred to as WWER [12,13], i.e. a water-cooled water-moderated energy reactor, or by the Russian transcription VVER. These are dual-circuit power plants where the nuclear part is referred to as the primary circuit. The primary circuit includes equipment for converting energy from nuclear decay to hydrothermal energy. This is then transferred to the thermal energy of steam in a steam generator. The primary circuit consists of a reactor, piping systems for water circulation, a steam generator, a volume compensator and circulation pumps.

In a broader sense, the process of decommissioning NPPs consists of administrative and technical operations, from the final decommissioning, through the removal of radioactive sources, to the subsequent decontamination and cleaning of the equipment. This is followed by the dismantling of structures and processing, storage and entombment of the radioactive waste. The comprehensive decommissioning process is completed by an investigation and release of space for further constructions. In practice, a limited number of the foregoing steps is referred to as decommissioning, with further steps (e.g. decontamination, dismantling) being deferred. These scenarios are formally referred to as: immediate decontamination and dismantling

* Corresponding author.
E-mail addresses: michal.stary@tul.cz (M. Starý), frantisek.novotny@tul.cz (F. Novotný), marcel.horak@tul.cz (M. Horák), marie.stara@tul.cz (M. Stará).

https://doi.org/10.1016/j.autcon.2020.103303
Received 10 July 2019; Received in revised form 25 May 2020; Accepted 1 June 2020

(DECON), safe storage (SAFESTOR), and entombment (or mothballing) [14].

The decontamination part of the decommissioning process includes, in addition to the decontamination procedure itself, control mechanisms in the form of thorough radiological monitoring of the decommissioned parts. Taking into account the nature of radioactive conversion, the issue of decontamination in NPPs focuses on activities performed in order to remove radioactive materials from the surfaces of contaminated equipment. Materials activated by neutron flux irradiation are not subject to decontamination, since the rate of nuclear transformation cannot be affected by chemical agents or normal physical procedures, and the radioactive material cannot be deprived of its properties.

The effectiveness of the decontamination [15–17] is assessed by the level of surface contamination, which indicates the radioactive decay in the area over time and the dose equivalent. Due to the variety of the forms of contamination, construction materials, surface quality and the requirements of maximum decontamination effectiveness with minimal generation of radioactive waste, it is clear that various different processes are used in the power plant. One of the most commonly used decontamination methods is chemical decontamination through mineral acid-based decontamination solutions. Contact with contaminated surfaces results in the dissolution of corrosion products such as heavy metal ions from alloy steel and the adherent radionuclides [18].

The subject of interest of the present article is the piping system of the primary circuit of an NPP, which is connected to the pressure vessel of the reactor. This is a hard-to-access and hazardous environment, especially due to the presence of radiation. Therefore, when collecting samples, it is necessary to use robotic systems.

Maintenance and inspection robots (MIRs) play a very important role in applications in the radiation environment of an NPP. These robots are designed specifically for the particular needs of the client, or platforms are modified from military or rescue environments. Therefore, they tend to be highly specialized and costly solutions. Currently, there are several such specific platforms, and a comprehensive and detailed overview of MIRs with an emphasis on their application and function is given in [19] or [20]. In most MIRs for radioactive environments, the conveyance subsystem is based on tracks [21–23] or wheels [24–26]. Alternative conveyance subsystems based on biological models, such as walking [27,28], snake-type [29,30] or climbing [31,32] systems, are less common.

The shape specifics of the working environment created by the piping system place specific requirements on the conceptual design of the proposed robotic systems. Therefore, it is logical to seek inspiration from MIRs used for conventional piping systems, where the conveyance is most commonly solved using a system of wheels [33–36], or tracks [37] spread over the respective pipe diameter. For example, if the robot is required to move vertically, then magnetic wheels [38,39] or systems with high adhesion [36] are applied. The application of MIRs for piping systems or at least their nozzles in a radioactive contamination environment is represented only by isolated cases [40,41].

The fundamental problem in the relevant field is the absence of standards [19] and the very limited and complicated possibilities for testing in radioactive environments, or simulated radioactive environments [42,43]. The radiation resistance of MIRs is usually proven through their operation, and additional adjustments of the equipment are very limited and difficult. Hence, the resulting radiation resistance of robots [44] is mainly defined by the experience of the respective design team. Examples of the unsuccessful deployment of MIRs in the context of complex post-disaster environments with strong radiation are demonstrated by robot applications in the Fukushima NPP [45].

From the point of view of effectors, most MIRs for radioactive environments are focused on inspection, i.e. they are equipped with monitoring and sensor technologies. Alternatively, they can be equipped with a gripper or a cutting, drilling, or grinding tool. Hence, the collection of contaminated samples from solid surfaces by means of robots represents a very unique role. From the given perspective, it is possible to mention sampling in other environments (especially rock), where highly invasive sampling probes are usually in the form of collection vessels attached to a cutting or drilling tool, or fragments created using a vibrating hammer are collected [46]. In the case of non-destructive or less-invasive methods, rotary brushes are usually used. An example is the dust removal tool [47], which is part of the Curiosity Rover.

2. Technical background

2.1. Situational description

The present robotic system is mainly designed for WWER-440-type NPPs, which are the most widespread type in Central and Eastern Europe and in Russia. The sampling is assumed in a straight section of the pipe in relation to the nozzles. The inside diameter of the primary pipe, which is the basic limiting factor for the design of the robot, is in this case 500 mm. For more powerful versions of similar types of NPPs, i.e. WWER-1000, 1200 and 1500, the pipe diameter is increased to 850 mm with respect to the coolant velocity and pressure loss [48–50]. The robot is designed with a view to easy modification of the platform for larger pipe diameters and is not limited solely to a specific type of NPP.

The collection of samples using a guided service robot is assumed after the decontamination solution is drained, i.e. in a relatively dry environment. The robot is guided to the pipeline by an auxiliary manipulation device, which is not a subject of the illustrated solution, or it can be modified to use the existing manipulation system of the respective NPP. The platform with the robot and an energy chain with power and information feeds from the robot control system located at a suitable location on the top of the reactor platform (Fig. 1) is placed on the manipulator. The mobile platform of the service robot allows the probe to be moved to a pre-selected position in the pipeline so that the achievable accuracy of the axis of the sampling point of the probe is better than a square with a side of ± 20 mm.

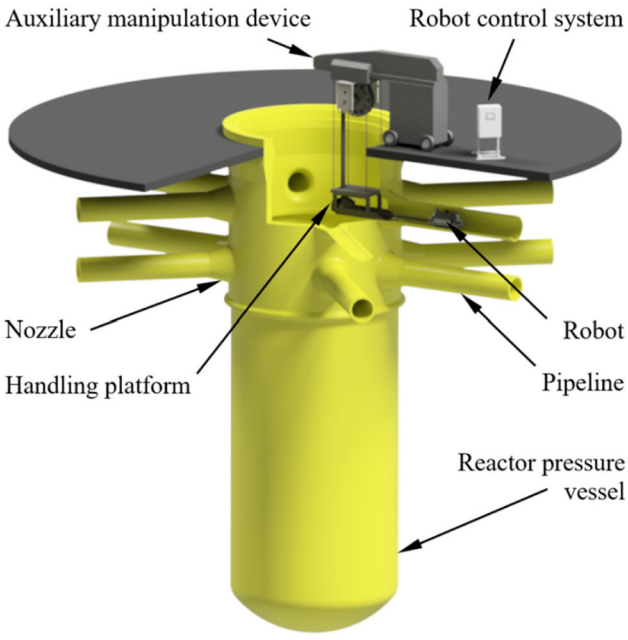

Fig. 1. Dispositional diagram of the robot application in a primary circuit of an NPP.

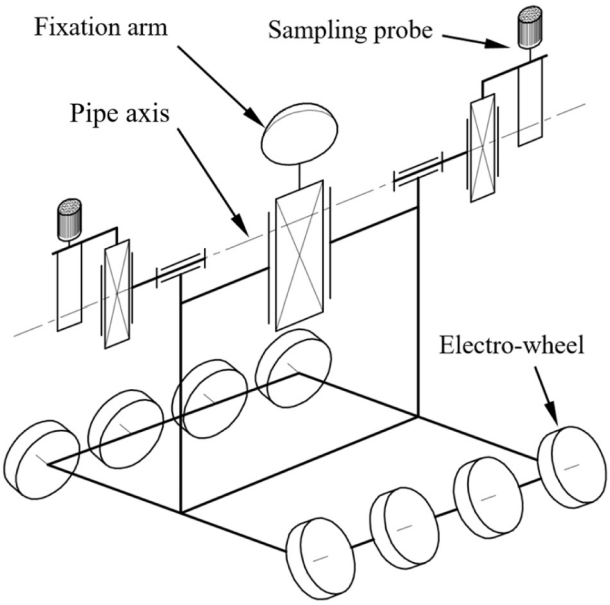

Fig. 2. Conceptual diagram of the robot design.

2.2. Robot concept

The basic concept of a DECOMOLER (DECOmmissioning MOLE Robot) is shown in Fig. 2. The conveyance device was designed in the form of a wheel system consisting of four independent pairs of wheels with an integrated drive in the axis of each wheel. The solution is a rugged yet simple option for the easy replacement of damaged wheels. The concept also allows for a relatively easy transition to a track system. A system of mechanical probes was chosen for the sampling, in order to maintain the possibility of analysing the composition of corrosion layers on the construction material. A total of two sampling probes are considered, one in the front and the other in the rear of the robot. For the sampling probes, a rotatable mounting located along the pipe axis is designed, which allows the tangency of the tool face to the surface to be examined to be maintained for any tilt angle. Stabilization of the robot in the pipeline during the sampling is ensured by a slide-out fixation arm.

3. Experiments and results

The experimental activity, the results of which served as an input for the design of the robot, focused on two basic areas – the sampling tool and the mobile platform. Testing of the sampling tool, which is a key element of the proposed system, focused on the design and operating parameters of the sampling tool. The mobile platform experiments were aimed at verifying the functionality and proper arrangement of the wheels.

3.1. Sampling tool

A logical base element of the sampling probe is a suitable tool. The essence of the material composition of the collection part of the brush is to avoid non-separable contamination of the sample being taken, i.e. the tool must not contain metal elements. An abrasive end brush was selected from a range of tools potentially available for sample collection based on the conducted research and applying the know-how of the investigators [51]. The filaments are attached to the flange of the tool using a two-component epoxy fixing material. The unique manufacturing process of the tool provides a high-quality tool head with evenly distributed filaments.

The most important parts of the brush are the filaments – the abrasive composite filaments with the desired properties. Polyetheretherketone (PEEK) was chosen as the carrier matrix material for the abrasive composite filaments with the synthetic diamond abrasive, which has higher mechanical strength, stiffness and heat resistance compared to most other thermoplastics. In addition, PEEK has excellent resistance to chemicals – acids, solvents and lubricants – even at high temperatures, which are undoubtedly the properties applicable during a quantitative evaluation of grinder dust, i.e. separation and release of dust from the filaments of the tool.

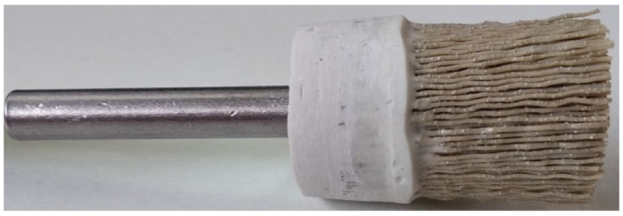

Fig. 3. Designed sampling tool.

The composite filaments with the synthetic diamond abrasive on a PEEK platform can be applied for the production of abrasive brushes with a range of parameters, of which the free length of the filaments [mm]; the filament diameter [mm]; the grain size of the diamond used [mesh]; the concentration of the used abrasive [%]; the filament geometry; the brush shape and diameter [mm] are decisive. Based on the experience of the tool manufacturer, previous work of the authors and targeted extensive experimental verification, which is not the subject of the present article, a sampling tool (Fig. 3) was designed with the following parameters:

- outer diameter of 20 mm;
- filament diameter of 0.4 mm;
- filament length of 20 mm;
- round crimped filaments;
- diamond grain size of 80 M;
- maximum possible diamond concentration at a level of 23%.

The tests were performed on a laboratory test stand (Fig. 4), which allowed for the verification of the proposed technological procedure of the sampling as well as the implementation of an experimental plan aimed at optimizing the cutting parameters. The basis of the measuring apparatus was a six-axis force-torque sensor, which was used to monitor the contact force and torque during the collection of a circular sample from the surface of a stainless-steel sheet. The set of samples was then used to check the technological properties of the brushes and to optimize their parameters, taking into account the quality and uniformity of the marks of abrasion, especially the ability to retain and then to separate the captured material sample easily and without any admixtures (metal contamination from the tool).

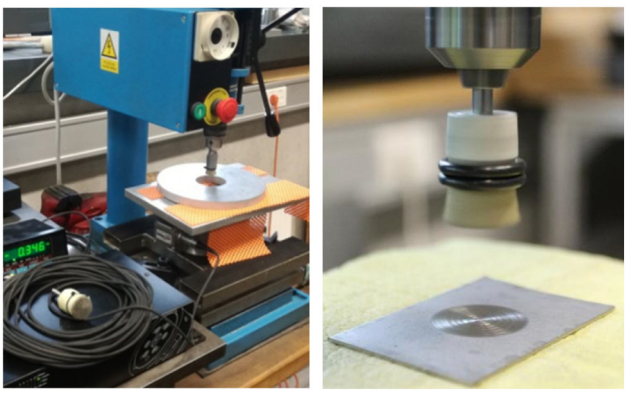

Fig. 4. Laboratory stand with a close-up of the final sampling tool.

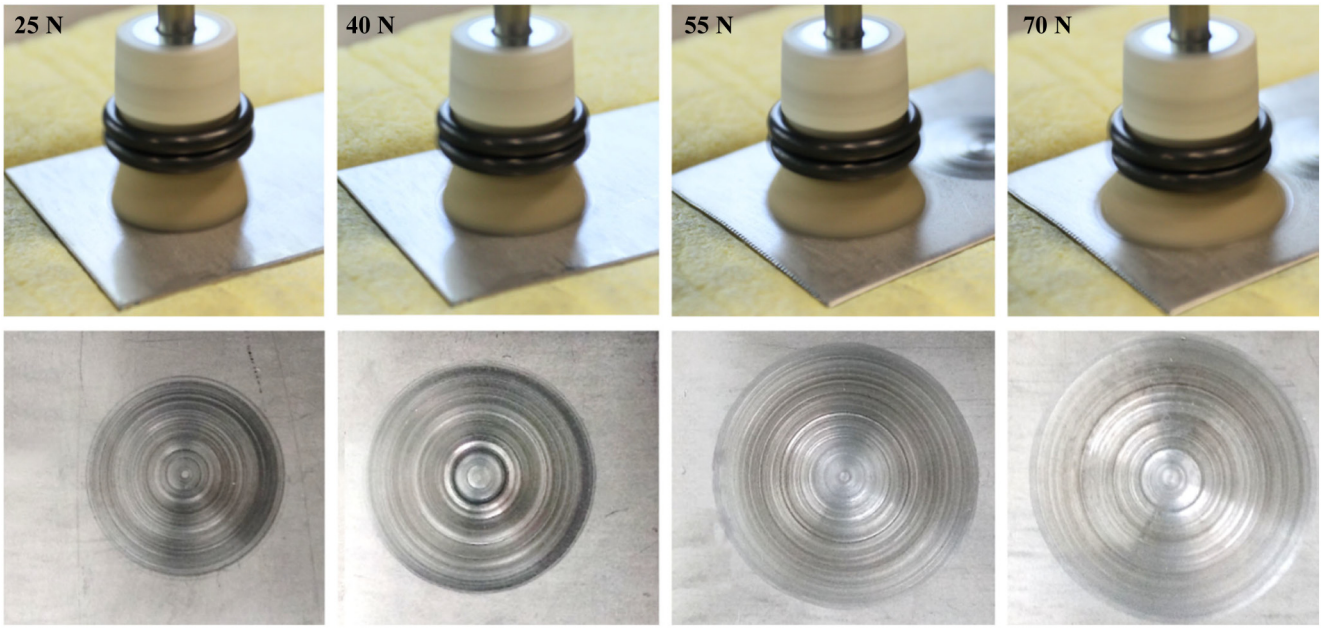

Fig. 5. Shape deformation of the sampling tool at various individual downforce levels and the corresponding abrasion marks.

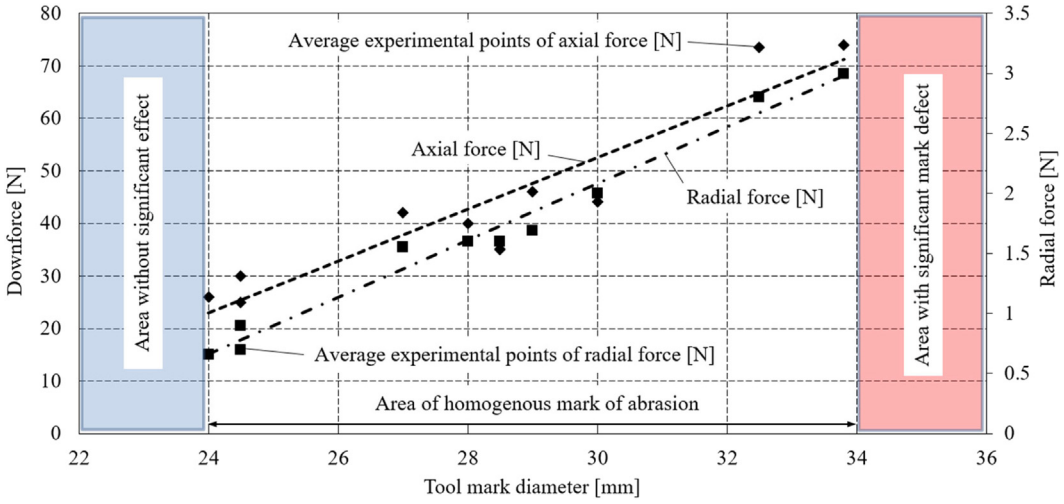

Fig. 6. Graph of optimum downforce levels.

The main operational parameter under investigation was the level of tool downforce. This was used to derive the abrasive effect of the tool as well as the associated deformation response of the filaments. With the level of downforce of the brush, its opening increases, which increases the abrasive effect of the filaments on the exposed surface. Research has shown that it is desirable for the tools to locally modify the stiffness and stability ratios of the filament bundle. By applying clamping elements in the heel region of the filament bundle, it was possible to achieve the desired stiffness of the filament bundle by varying the tool downforce. The application of two elastomeric o-rings with a suitable cross-section proved to be optimal (Fig. 4). The modification of the tool increased the stiffness of the filaments in the sense of opening the brush and, in contrast to the fixed or pseudo-rigid placement (e.g. application of a tightening belt), the remaining filaments were sufficiently flexible in the sense of rotation, i.e. the torsion of the tool. With the appropriate modification, the optimum progressive conical shape of the tool was achieved under load, see Fig. 5, thereby achieving desensitization of the tool to the downforce level. A suitable downforce level was set in the range of approximately 25 to 70 N (Fig. 6), which corresponds to an infeed of approximately 2 to 8 mm. At a lower downforce, the tool loses its abrasive function and, on the other hand, a significant deformation of the filaments occurs at higher downforce, whereby causing significant mark defects on the surface.

The second operating parameter was the tool speed. This was chosen with a view to ensuring the intensive cutting (abrasive) function of the tool in contrast to the requirement to keep the grinder dust inside the brush. The level of intensity of the abrasion with regard to the running of the tool in a dry mode must be chosen so that the abrasive filaments are not damaged. The upper level of the tool speed is also limited by the requirement to maintain as much grinder dust in the tool as possible while minimizing the emission of grinder dust to the environment due to the effect of centrifugal force. Generally, for the abrasive end brush with a diameter of 20 mm, manufacturers recommend a speed of 3000, or 4000 to 20,000 rpm [52,53]. Taking into account the technical capabilities of the test stand being limited to 3000 rpm, the tests were performed at the given maximum speed. Reducing the speed resulted in a significant decrease in the brush abrasion.

The third investigated factor associated with the above-mentioned operating parameters was the brush yield. The principle of the tests was

to compare the measured amount of grinder dust with the weight of the samples taken. The total amount of grinder dust was determined based on the chemical analysis of the digest and the knowledge of the chemical composition of the steel samples. The weight of the samples taken during the test was determined gravimetrically using calibrated analytical scales with a sensitivity of 0.01 mg. Direct determination based on the difference in weight of the brushes before and after exposure could not be used with respect to the undefined abrasion of the actual brush mass. It can be stated that the results within the declared optimal working range show a yield in the range of approximately 60 to 80%.

3.2. Mobile platform

The development of the mobile platform was preceded by calibration of the wheels to achieve the optimum analogue output so that a series of four wheels (on the left and right sides of the robot) operated at the same rotational frequency and avoided mechanical problems due to slippage of some of the wheels. Subsequently, the development of the mobile platform could begin, which primarily consisted of wheel alignment tests. The aim was to obtain an arrangement that ensures the self-levelling function of the mobile platform while maintaining the ability of the mobile platform to move on a horizontal surface. Moreover, a series of simple wheel set-ups was designed in the appropriate arrangement, i.e. at 90°, 75°, 60° and 45°, see Fig. 7. In addition, a set of three test troughs, each measuring one meter in length, corresponding to the respective pipe diameter, were made for this purpose.

The experimental verification of the mobile platform involved the placement of the mobile platform in the trough in a tilted position and monitoring whether and at what distance the self-alignment would occur. Each experiment was repeated 10 times. The experiments showed that the optimal wheel arrangement for the trough movement was 45°. Higher inclination of the wheels led to a reduction in the auto-stabilizing ability of the mobile platform, which is very important for the application. In the case of a 90° slope, the effect was most noticeable, i.e. the mobile platform remained in its initial tilted position throughout the movement (Fig. 8). In contrast, Fig. 9 demonstrates the ability of the mobile platform to quickly stabilize its orientation on a mobile platform with wheels below 45°. The full self-alignment of this mobile platform occurred at a distance of approximately 1 ± 0.1 m.

4. Robot design

The robot (Fig. 10) can be divided into a set of functional units – mobile platform, slide-out fixing arm and sampling probes. The robot is also equipped with a pneumatic circuit, the elements of which are described within the above-mentioned functional units. Furthermore, the robot is equipped with sensors and a control system. Most of the designed prototype components are made of an aluminium alloy. The total weight of the robot is 72 kg. The movement speed can be controlled in the range of approximately 0.2 to 1 m/s.

4.1. Mobile platform

The mobile platform is made up of a supporting plate, which is fitted from the lower part with a module of control units of the conveyance wheels and bearing segments, in which reversible wheels with integrated brushless DC drive with a maximum output of 200 W (24 V) are placed. The wheels are torus-shaped with a diameter of 105 mm. The upper part of the mobile platform is fitted with parallel plates with spacers defining the space for the installation of additional modules and components, such as an autonomous media source for the pneumatic circuit (two 2-litre tanks of compressed air). A vertical fixing arm, which is firmly tied to the mobile platform, then passes through the centre of the top of the mobile platform.

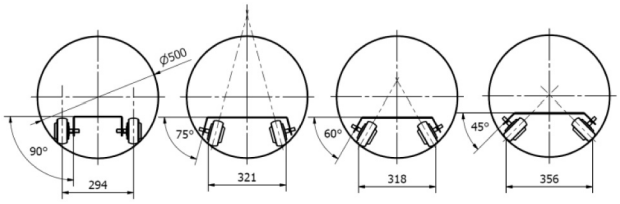

Fig. 7. Overview of the mobile test platforms.

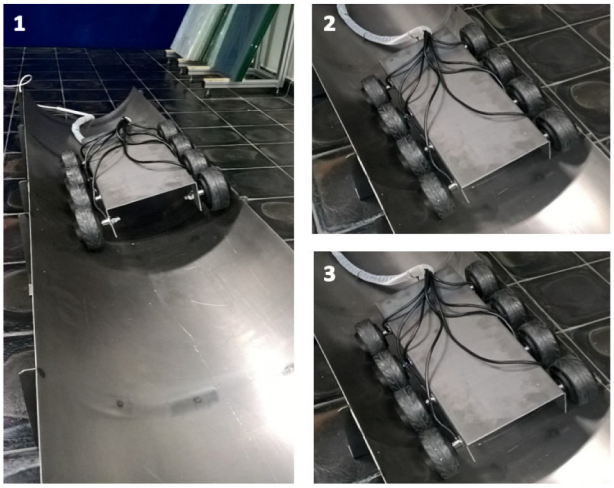

Fig. 8. Demonstration of a mobile platform test with wheels below 90°.

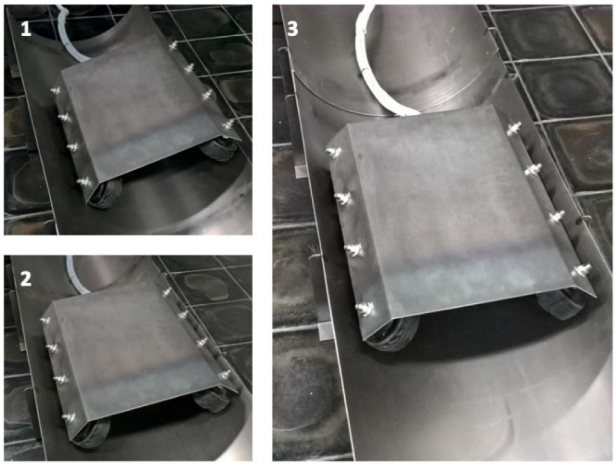

Fig. 9. Demonstration of a mobile platform test with wheels below 45°.

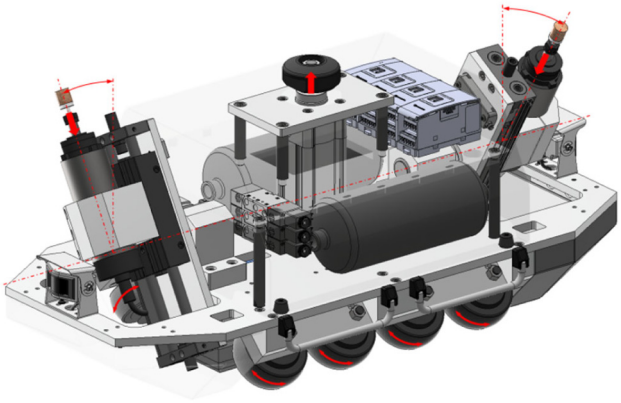

Fig. 10. Model of the robot (transparent cover).

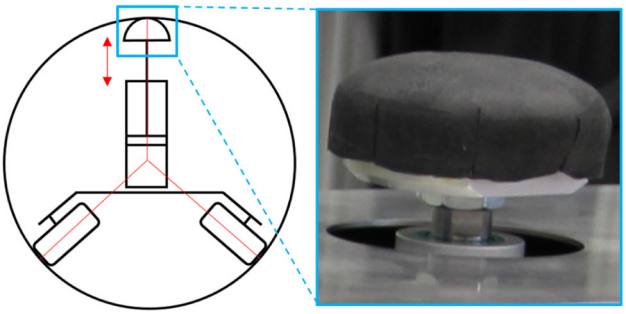

Fig. 11. Schematic diagram of the mobile platform and fixing arm with a close-up of the stopper.

4.2. Slide-out fixing arm

The slide-out fixing arm helps ensure the stability and fixed positioning of the robot during the sampling. The slide-out movement is provided by means of a pneumatic cylinder. The piston rod of the cylinder is ended by a mushroom-shaped stopper. The surface of the stopper is equipped with an elastomeric layer in order to increase the frictional properties (see the close-up image in Fig. 11). The proposed concept builds on from the self-levelling form of the platform, i.e. the shape of the stop and the absence of an auxiliary guide for the pneumatic cylinder minimize the additional forces generated by inaccurate alignment of the platform in the trough. The central arrangement of the slide-out fixing arm, along with the straddled mobile platform design, i.e. the configuration of the wheels below 45°, form a 'Y' shape (Fig. 11), ensuring sufficient stability of the fixing of the platform in the pipeline.

4.3. Sampling probe

The front and rear of the robot are equipped with swivel arms with linear units on which the sampling probes are located. The sampling probes consist of a sampling tool clamped by a shank (see Fig. 12) in a spindle chuck with an electric drive. The axial movement of the sampling tool, providing the feed and downforce, is generated by the linear unit with pneumatic drive. Primarily, with regard to the exact shape and dimension of the pipeline, position control linked to the stopper settings is assumed, but it is also possible to use a force control method by means of pressure in the pneumatic circuit. The probe is mounted on the clamping pin with the possibility to adjust the rotation about the pipe axis by ± 32° so that when the sampling probe is rotated, the movement of the sampling tool is radial. In this way, for each selected position of the sampling probe axis, a uniform pressure of the sampling tool is ensured on the pipe surface during the sampling. The speed of the spindle can be set from 3000 to 8000 rpm. The maximum torque is 10 Nm.

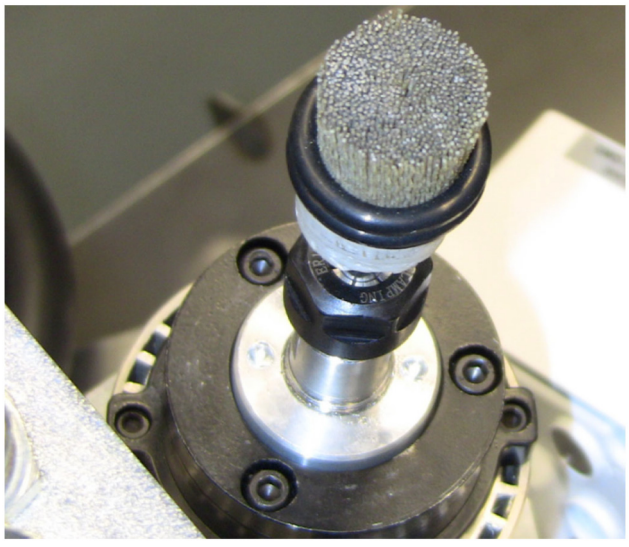

Fig. 12. Close-up of the sampling tool fitted into the spindle.

A higher level of residual contamination can be assumed in the upper part of the pipeline taking into account the decontamination process technology, and therefore the sampling probes are set in this area. Alternatively, the sampling probes can be turned upside down in order to take samples from the bottom of the pipe.

4.4. Sensor system

Before and after decontamination, samples must be taken in the same manner and from a similar place in the pipeline to evaluate the effectiveness of the decontamination and to perform the secondary radioactive waste balance. There are several ways of locating the sampling point. The distance in the pipeline is monitored by a wire sensor. The sensor body with a winding drum is placed on the handling platform and the end of the wire is attached to the robot. Furthermore, the inclination of the robot around the pipe axis is monitored by three inclination sensors. One is directly on the robot chassis and the other two are on the sampling probes.

An additional sensor system can be considered to be a static low-cost camera system with infrared illumination located on the front and rear of the robot.

4.5. Electrical control system

The robot control system was designed on a programmable logic controller (PLC) platform in combination with digital and analogue input/output modules.

In order to minimize the voltage drop due to the length of the conductor and the number of core wires of the flexible supply cable, the system was divided into two parts. The processor part of the control is installed in a stationary distribution box together with a voltage source, protection system and other electrical wiring components. The switchboard is also complemented by a frequency converter to control independently mounted spindles mounted on the robot chassis. To increase the user-comfort when controlling the basic functions of the robot, the PLC is complemented by a colour touch-screen HMI panel and a wireless communication interface for remote system management. On the side of the robot are control units for controlling the wheels. In the upper part of the mobile platform there are the input and output modules, which are used to control the wheels and the electro-pneumatic valves for positioning the pneumatic cylinders etc.

It is assumed that the robot controls will be in the "non-radiation" zone and the connection with the robot will be made by a multi-core flexible shielded cable with a length of approximately 30 m.

5. Prototype testing

The robot prototype was successfully subjected to a series of tests aimed at verifying the functionality of the sub-modules as well as the entire system (Fig. 13).

The conveyance functions in the test trough and the pipeline were verified both under completely dry conditions and with modified surface conditions in the form of an applied film of water. The control and guidance functions were also tested by repeating the approach to the same position. Furthermore, the ability to stabilize the robot in the pipeline in order to ensure stable sampling was examined. The main emphasis was placed on verifying the functionality of the robot during the sampling (Fig. 14). Full compressed air tanks were found to be sufficient for four sampling cycles, which represents a 100% reserve for the given solution in the form of two sampling probes. The sampling

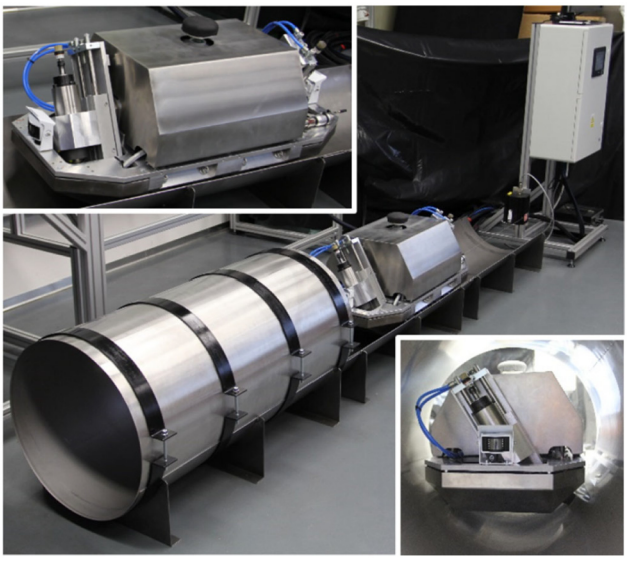

Fig. 13. Photo documentation of the robot tests.

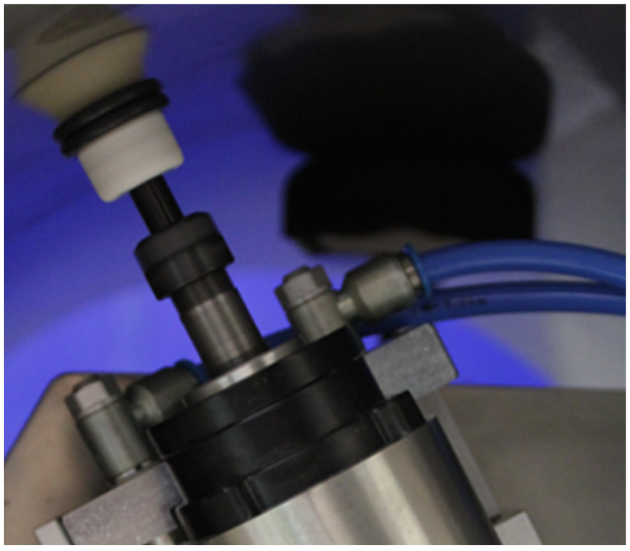

Fig. 14. Photo documentation of sampling in the pipe.

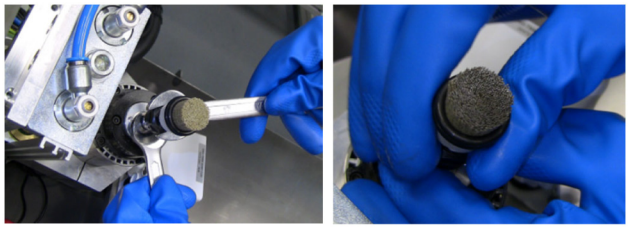

Fig. 15. Assembling and disassembling the sampling tool from the sampling probe.

time does not affect the compressed air consumption for the given solution. The researchers also focused on manipulation of the sampling tool, i.e. its removal from the spindle, which is released by two spanners (Fig. 15). The sampling tool can be removed either by grasping the brush at the bottom of the head, or by inserting an auxiliary fork under the head of the loosened tool, pulling it out and then grasping the tool shank.

Attention was also paid to verifying the functionality of the sampling probe on a pseudo-real pipeline. The inner surface of the piping of an exposed primary circuit was formed by a spinel corrosion layer [54,55]. Due to the difficult accessibility to and complicated handling of samples of real corrosion layers of the primary circuit, a method of artificial preparation of the corrosion layer (Ni0.1Fe0.45Cr0.45)3O4 was developed by UJV ŘEŽ for this analytical procedure, including the method of its application on the surface of the cylindrical pipe model. The known composition of the corrosion layer enabled the verification of the analytical procedure, which involves extracting the dust from the sampling tool filaments and subsequently performing a chemical analysis of the dust. The normal sampling time was selected at 5–10 s, which corresponds to a grinder dust yield of more than 3 mg per sampling tool. Due to the nature of the process, i.e. contamination of the tool during retraction, it is not possible to reuse it. So it is a low-cost (about 30 €) disposable tool.

6. Discussion

The robot for collecting samples from a primary circuit pipeline of an NPP described in the article, is a realistic concept for determining the success of the decontamination process. This has become a useful basis for building the knowledge base of the decommissioning process. The functional sample of the robot and the sampling probe was designed with an emphasis on achieving the desired function; however, it will still be necessary to solve the resistance of the robot to radiation exposure for real deployment in an NPP.

Due to contamination of the robot, it is assumed that the device will be permanently deployed in the selected NPP. Primarily, it is anticipated that it will be possible to use it within the Czech Republic at NPP Dukovany 1-4, with currently planned closure around 2035, or in the Slovak Republic in Jaslovské Bohunice 1-4, where the first two units are already shut down and the other two are scheduled to close in 2025.

7. Conclusion

The article presents a successful design and modification of the DECOMOLER robotic system designed to identify the initial contamination from the most difficult to access surface, i.e. the inside of the reactor core circuit, and to evaluate the effectiveness of the decontamination process. The robot is controlled from a safe distance in an environment that does not endanger the operator's life. The basis of the article is the sampling probe in the form of an abrasive brush. The main findings and choices of the proposed low-cost technical solution can be summarized as follows:

- The robot is fully capable of moving in a straight line and repeatedly reaching the target position with an accuracy of tens of mm.
- The proposed technical solution provides a fixed positioning of the robot in the piping with a diameter of approximately 500 mm and stable sampling of two samples.
- A mechanical probe with a replaceable tool is designed for sampling and analysis of the composition of contamination residues on the primary pipe.
- The optimum technical and operational parameters of the sampling tool were determined, the yield of which is 60 to 80% of the abraded material, which is a sample of approximately 3 mg.
- Removal of the contaminated tools from the robot's sampling probes is assumed by a simple manual operator action.

Further development will be necessary for real deployment, which will involve increasing the radiation resistance of the equipment. This is particularly true for the functional plastic parts in the pneumatic components, i.e. seals. Default selected polyurethane polymer has a relatively high radiation resistance, however, it can be a challenge to find and test a more suitable material for a given application. Alternatively, the number of electrical components should be minimized. The selected modules, such as sampling probe spindles, might be

replaced with pneumatic drive motors with a quick-release system of tools.

It is assumed that in the next phase of development, the robot will be equipped with an anti-radiation shield to protect the electrical engineering against damage and interference. The appropriate choice of shield material remains still a question. Most probably it should be based on lead or a modern trend in the form of glass-ceramics with heavy metals. Also, the integrity and IP of the components used will be modified to improve the robot resistivity to the decontamination spray.

When selecting the components, emphasis was placed on simplicity and low acquisition costs. It is assumed that instead of increasing the radiation resistance of some of the components (e.g. the cameras and their glass lenses), a limited lifespan will be calculated and the components will be replaced more frequently.

Declaration of competing interest

The authors declare that they do not have any commercial or associative interest that represents a conflict of interest in connection with the work submitted.

Acknowledgement

The results were obtained with co-funding from *the project* Knowledge Basis for Decommission of Nuclear Energy Facility (Reg. No.: CZ.01.1.02/0.0/0.0/15_019/0004507) financed by the Ministry of Industry and Trade of the Czech Republic as part of the Operational Programme Business and Innovation for Competitiveness. It was also supported by the Ministry of Education, Youth and Sports, within Institutional Support for Long-Term Development of Research Organizations – Technical University of Liberec, Faculty of Mechanical Engineering.

References

[1] International Atomic Energy Agency, Nuclear power reactors in the world, reference data series no. 2, IAEA, Vienna, (2018) Available at https://www-pub.iaea.org/MTCD/Publications/PDF/RDS-2-38_web.pdf , Accessed date: 30 January 2020.

[2] Nuclear energy agency, Nuclear power plant life management and longer-term operation, NEA No. 6105, OECD, Paris, (2006) Available at https://www.oecd-nea.org/ndd/pubs/2006/6105-npp-life-management.pdf , Accessed date: 30 January 2020.

[3] K. Tweed, APS argues to extend lifespan of nuclear reactors to 80 years, IEEE Spectrum, 2013 Available at https://spectrum.ieee.org/energywise/energy/nuclear/aps-argues-to-extend-lifespan-of-nuclear-reactors-to-80-years , Accessed date: 30 January 2020.

[4] G. Rothwell, J. Rust, On the optimal lifetime of nuclear power plants, J. Bus. Econ. Stat. 15 (1997) 195–208, https://doi.org/10.1080/07350015.1997.10524700.

[5] S. Nemytov, V. Zimin, NPP decommissioning: the concept; state of activities, International Meeting 'Nuclear Power in Eastern Europe: Safety, European Integration, Free Electricity Market' and The Tenth Anniversary of Bulgarian Nuclear Society, Varna, 2001 Available at https://inis.iaea.org/collection/NCLCollectionStore/_Public/32/057/32057857.pdf?r=1&r=1 , Accessed date: 30 January 2020.

[6] B. Brendebach, Decommissioning of nuclear facilities: Germany's experience, IAEA Bull. 57 (2016) 24–25. Available at https://www.iaea.org/newscenter/news/decommissioning-of-nuclear-facilities-germanys-experience , Accessed date: 30 January 2020.

[7] R. Volk, F. Hübner, T. Hünlich, F. Schultmann, The future of nuclear decommissioning – a worldwide market potential study, Energy Policy 124 (2019) 226–261, https://doi.org/10.1016/j.enpol.2018.08.014.

[8] A. Baecker, Decommissioning of Russian-type water-cooled water-moderated nuclear reactors (WWERs), in: M. Laraia (Ed.), Nuclear Decommissioning, Woodhead Publishing Series in Energy, Cambridge, 2012, pp. 564–606, , https://doi.org/10.1533/9780857095336.3.564.

[9] M. Laraia, Overview of nuclear decommissioning principles and approaches, in: M. Laraia (Ed.), Nuclear Decommissioning, Woodhead Publishing Series in Energy, Cambridge, 2012, pp. 13–32, , https://doi.org/10.1533/9780857095336.1.13.

[10] B. Volkmann, U. Löschhorn, Aspects on decommissioning of the Greifswald nuclear power plant, Nucl. Eng. Des. 159 (1995) 117–121, https://doi.org/10.1016/0029-5493(95)01071-O.

[11] P. Breeze, Chapter 4 - water-cooled reactors, in: P. Breeze (Ed.), Nuclear Power, Academic Press, Cambridge, 2017, pp. 33–44, , https://doi.org/10.1016/B978-0-08-101043-3.00004-3.

[12] E. Narkunas, G. Poskas, A. Smaizys, Impact of shield elements on the WWER-440 reactor pressure vessel activation, Ann. Nucl. Energy 130 (2019) 394–401, https://doi.org/10.1016/j.anucene.2019.03.008.

[13] V.G. Asmolov, I.N. Gusev, V.R. Kazanskiy, V.P. Povarov, D.B. Statsura, New generation first-of-the kind unit – VVER-1200 design features, Nucl. Energy Technol. 3 (2017) 260–269, https://doi.org/10.1016/j.nucet.2017.10.003.

[14] Y.A. Suh, C. Hornibrook, M.-S. Yim, Decisions on nuclear decommissioning strategies: historical review, Prog. Nucl. Energy 106 (2018) 34–43, https://doi.org/10.1016/j.pnucene.2018.02.001.

[15] Z. Nemeth, et al., Comparative study of the corrosion and surface chemical effects of the decontamination technologies, J. Radioanal. Nucl. Chem. 286 (2010) 815–821, https://doi.org/10.1007/s10967-010-0761-8.

[16] M. Pražská, J. Rezbárik, M. Solčányi, R. Trtílek, Actual situation on the field of decontamination in Slovak and Czech NPPs, Czechoslov. J. Phys. 53 (2003) A687–A697, https://doi.org/10.1007/s10582-003-0088-6.

[17] L. Noynaert, Decontamination processes and technologies in nuclear decommissioning projects, in: M. Laraia (Ed.), Nuclear Decommissioning, Woodhead Publishing Series in Energy, 2012, pp. 319–345, , https://doi.org/10.1533/9780857095336.2.319.

[18] R. Morris, Chemical decontamination for decommissioning (DFD) and DFDX, 13th International Conference on Environmental Remediation and Radioactive Waste Management, ASME, Tsukuba, 2011, pp. 267–272, , https://doi.org/10.1115/ICEM2010-40007.

[19] I. Tsitsimpelis, C.J. Taylor, B. Lennox, M.J. Joyce, A review of ground-based robotic systems for the characterization of nuclear environments, Prog. Nucl. Energy 111 (2019) 109–124, https://doi.org/10.1016/j.pnucene.2018.10.023.

[20] F. Zhao, Y. Ma, Y. Sun, Application and standardization trend of maintenance and inspection robot (MIR) in nuclear power station, 3rd International Symposium on Mechatronics and Industrial Informatics, DEStech Publications, Haikou, 2017, , https://doi.org/10.12783/dtetr/ismii2017/16678.

[21] F.E. Gelhaus, H.T. Roman, Robot applications in nuclear power plants, Prog. Nucl. Energy 23 (1990) 1–33, https://doi.org/10.1016/0149-1970(90)90012-T.

[22] J. Abouaf, Trial by fire: teleoperated robot targets Chernobyl, IEEE Comput. Graph. Appl. 18 (1998) 10–14, https://doi.org/10.1109/38.689654.

[23] A. Iborra, J.A. Pastor, B. Alvarez, C. Fernandez, J.M.F. Merono, Robot in radioactive environments, IEEE Robot. Autom. Mag. 10 (2003) 12–22, https://doi.org/10.1109/MRA.2003.1256294.

[24] F.L. Schwartz, R.D. Meininger, TMI-2 experience with remote operations technology, in: G.A. Tarcza (Ed.), International Decommissioning Symposium, IAEA, Pittsburgh, 1987, pp. VI14–VI28. Available at https://tmi2kml.inl.gov/Documents/10a-Decon/DOE-C0NF-87101B-V2,%20Proceedings%20of%20the%201987%20International%20Decommissioning%20Symposium%20(1987-10).pdf , Accessed date: 30 January 2020.

[25] C.J. Hess, S.W. Metzger, Steady progress at TMI-2, IAEA Bull. 27 (1985) 16–22. Available at https://www.iaea.org/sites/default/files/27404691622.pdf , Accessed date: 30 January 2020.

[26] S. Kim, S.H. Jung, S.U. Lee, C.H. Kim, H.C. Shin, Y.C. Seo, et al., Application of robotics for the nuclear power plants in Korea, 1st International Conference on Applied Robotics for the Power Industry, IEEE, Montreal, 2010, pp. 1–5, , https://doi.org/10.1109/CARPI.2010.5624417.

[27] Y. Ichikawa, N. Ozaki, K. Sadakane, A hybrid locomotion vehicle for nuclear power plants, IEEE Trans. Syst. Man Cybern. 13 (1983) 1089–1093, https://doi.org/10.1109/TSMC.1983.6313182.

[28] J. Savall, A. Avello, L. Briones, Two compact robots for remote inspection of hazardous areas in nuclear power plants, Proceedings 1999 IEEE International Conference on Robotics and Automation, IEEE, Detroit, 1999, pp. 1993–1998, , https://doi.org/10.1109/ROBOT.1999.770400.

[29] C.-W. Huang, C.-H. Huang, Y.-H. Hung, C.-Y. Chang, Sensing pipes of a nuclear power mechanism using low-cost snake robot, Adv. Mech. Eng. 10 (2018) 1–8, https://doi.org/10.1177/1687814018781286.

[30] J. Falconer, CMU's snake robot explores defunct nuclear power plant, New Atlas, (2013) Available at https://newatlas.com/cmu-snake-robot-explores-nuclear-power-plant/28235/ , Accessed date: 30 January 2020.

[31] M.S. Rowland, M.A. Holliday, J.A. Karpachov, A. Ivanov, Proposed radiation hardened mobile vehicle for Chernobyl dismantlement and nuclear accident response, 6th Topical Meeting on Robotics and Remote Systems, American Nuclear Society, Monterey, 1995 Available at https://digital.library.unt.edu/ark:/67531/metadc664949/m2/1/high_res_d/238462.pdf , Accessed date: 30 January 2020.

[32] B.L. Luk, S. Galt, D.S. Cooke, N.O. Hewer, Intelligent walking motions and control for a legged robot, European Control Conference, IEEE, Karlsruhe, 1999, pp. 4756–4761, , https://doi.org/10.23919/ECC.1999.7100087.

[33] A. Kakogawa, S. Ma, Mobility of an in-pipe robot with screwdrive mechanism inside curved pipes, IEEE International Conference Robotics and Biomimetics, IEEE, Tianjin, 2010, pp. 1530–1535, , https://doi.org/10.1109/ROBIO.2010.5723557.

[34] P. Li, S. Ma, B. Li, Y. Wang, Development of an adaptive mobile robot for in-pipe inspection task, International Conference on Mechatronics and Automation, IEEE, Harbin, 2007, pp. 3622–3627, , https://doi.org/10.1109/ICMA.2007.4304148.

[35] D. Lee, J. Park, D. Hyun, G. Yook, H. Yang, Novel mechanisms and simple locomotion strategies for an in-pipe robot that can inspect various pipe types, Mech. Mach. Theory 56 (2012) 52–68, https://doi.org/10.1016/j.mechmachtheory.2012.05.004.

[36] L.A. Mateos, M. Vincze, DeWaLoP in-pipe robot embedded system, IFAC Proc. Vol. 45 (2012) 842–847, https://doi.org/10.3182/20120905-3-HR-2030.00122.

[37] Y.-S. Kwon, B.-J. Yi, Design and motion planning of a two-module collaborative indoor pipeline inspection robot, IEEE Trans. Robot. 28 (2012) 1–16, https://doi.org/10.1109/TRO.2012.2183049.

[38] M.R.A.M. Zin, K.S.M. Sahari, J.M. Saad, A. Anuar, A.T. Zulkarnain, Development of

a low cost small sized in-pipe robot, Procedia Eng. 41 (2012) 1469–1475, https://doi.org/10.1016/j.proeng.2012.07.337.
[39] F. Tache, W. Fischer, R. Siegwart, R. Moser, F. Mondada, Compact magnetic wheeled robot with high mobility for inspecting complex shaped pipe structures, IEEE/RSJ International Conference Intelligent Robots and Systems, IEEE, San Diego, 2007, pp. 261–266, , https://doi.org/10.1109/IROS.2007.4399116.
[40] K. Nagaya, T. Yoshino, M. Katayama, I. Murakima, Y. Ando, Wireless piping inspection vehicle using magnetic adsorption force, IEEE/ASME Trans. Mechatron. 17 (2012) 472–479, https://doi.org/10.1109/TMECH.2011.2182201.
[41] H. Rodriguez, T. Sattar, J. Shang, Underwater wall climbing robot for nuclear pressure vessel inspection, International Conference on Climbing and Walking Robots, World Scientific, Coimbra, 2008 Available at https://openresearch.lsbu.ac.uk/item/87q7v , Accessed date: 30 January 2020.
[42] H. Igarashi, K. Kon, F. Matsuno, Evaluation of sensors for mobile robots based on irradiation experiment, 2012 IEEE/SICE International Symposium on System Integration, Fukuoka, 2012, pp. 517–522, , https://doi.org/10.1109/SII.2012.6427382.
[43] K. Nagatani, S. Kiribayashi, Y. Okada, et al., Emergency response to the nuclear accident at the Fukushima Daiichi Nuclear Power Plants using mobile rescue robots, J. Field Robot. 30 (2013) 44–63, https://doi.org/10.1002/rob.21439.
[44] P.C. Bennett, L.D. Posey, RHOBOT: radiation hardened robotics, Sandia report, Sandia National Laboratories, Albuquerque, (1997) Available at https://prod-ng.sandia.gov/techlib-noauth/access-control.cgi/1997/972405.pdf , Accessed date: 30 January 2020.
[45] M.-A. Russon, Fukushima: robot 'dies' 3 hours after entering Japan's radioactive reactor, International Business Times, (2015) Available at https://www.ibtimes.co.uk/fukushima-robot-dies-3-hours-after-entering-japans-radioactive-reactor-1496126 , Accessed date: 30 January 2020.
[46] J. Brooks, M. Cantor, M. Ickowski, S. Simeonides, H. Stidham, A.V. Soto, The chip 'n' ship: a prototype rock chip sampling tool for use on microgravity bodies, Explorations 11 (2016) 77–91. Available at https://uncw.edu/csurf/explorations/volume%20xi/brooks%20et%20all.pdf , Accessed date: 30 January 2020.
[47] Jet Propulsion Laboratory, Sampling system, NASA, La Cañada Flintridge, Available at https://msl-scicorner.jpl.nasa.gov/samplingsystem/ , Accessed date: 30 January 2020.
[48] International Atomic Energy Agency, Status report 93 – VVER-1000 (V-466B) (VVER-1000 (V-466B)), IAEA, Vienna, (2011) Available at https://aris.iaea.org/PDF/VVER-1000(V-466B).pdf , Accessed date: 30 January 2020.
[49] International Atomic Energy Agency, Status report 108 – VVER-1200 (V-491) (VVER-1200 (V-491)), IAEA, Vienna, (2011) Available at https://aris.iaea.org/PDF/VVER-1000(V-466B).pdf , Accessed date: 30 January 2020.
[50] International Atomic Energy Agency, Status report 85 – VVER-1500 (V-448) (VVER-1500 (V-448)), IAEA, Vienna, (2011) Available at https://aris.iaea.org/PDF/VVER-1500(V-448).pdf , Accessed date: 30 January 2020.
[51] F. Novotný, M. Horák, M. Starý, Abrasive cylindrical brush behaviour in surface processing, Int. J. Mach. Tools Manuf. 118-119 (2017) 61–72 https://doi.org/10.1016/j.ijmachtools.2017.03.006.
[52] Weiler, Automated deburring with brushes, Weiler corporation, (2016) Available at https://www.weilerabrasives.com/UserFiles/Resources/Products/WC/38/6_/WC386_Auto_Deburring_Brochure_D.pdf , Accessed date: 30 January 2020.
[53] Osborn, ATB - abrasive brush tools, Osborn, (2013) Available at https://www.osborn.com/acNET_US/documents/ATBCatalog.pdf , Accessed date: 30 January 2020.
[54] K.-H. NEEB, The Radiochemistry of Nuclear Power Plants With Light Water Reactors, De Gruyter, Berlin, 1997, https://doi.org/10.1515/9783110812015 ISBN 978-3-11-081201-5.
[55] V.A. Kurepin, D.A. Kulik, A. Hiltpold, M. Nicolet, Thermodynamic modelling of Fe-Cr-Ni- spinel formation at the light-water reactor conditions, PSI Bericht 02-04, Paul Scherrer Institute, Villigen, (2002) Available at https://inis.iaea.org/collection/NCLCollectionStore/_Public/33/045/33045406.pdf?r=1&r=1 , Accessed date: 30 January 2020.